Available online at www.qu.edu.iq/journalcm
JOURNAL OF AL-QADISIYAH FOR COMPUTER SCIENCE AND MATHEMATICS
ISSN:2521-3504(online) ISSN:2074-0204(print)

Analyze a temperature and MHD peristaltic flow of sutterby fluid through a porous wavechannel in a rotating frame

Fatima Khalid Moean[a], Dheia G. Salih Al-Khafajy[b] *

[a]*Department of Mathematics, College of Science, University of Al-Qadisiyah, Diwaniya, Iraq. Email:* fatimakhalid19981116@gmail.com

[b]*Department of Mathematics, College of Science, University of Al-Qadisiyah, Diwaniya, Iraq. Email:* dheia.salih@qu.edu.iq

ARTICLE INFO

Article history:
Received: 5 /2/2024
Rrevised form: 16 /3/2024
Accepted : 24 /3/2024
Available online: 30 /3/2024

Keywords:

Porous wavechannel, Sutterby Fluid, Rotation, Magnetohydrodynamic (MHD).

ABSTRACT

The aim of this paper is to analyze the temperature and magnetohydrodynamic (MHD) peristaltic flow of non-Newtonian Sutterby fluid through a porous wavechannel under the influence of rotation. The problem formula is non-linear and non-homogeneous partial differential equations. By using the perturbation technique, we solved the momentum equation under the assumptions of a long wavelength and an extremely low Reynolds number. After getting the solution, we have used the "Mathematica 13" program to analyze the results through graphs, and it have been studied the effect of the rotation, magnetic field, viscosity of the fluid and average radius of the tube on the fluid movement and its temperature.

MSC..

https://doi.org/10.29304/jqcsm.2024.16.11447

1. Introduction

In industrial and physiological processes, the non-Newtonian fluids are acknowledged more than viscous fluids. There are several types of non-Newtonian substances that can be seen in nature such like shampoo, paints, ketchup and blood, Sutterby fluid model (which is a non-Newtonian fluid) represents the high-polymer aqueous solutions [6]. Porous media can be distinguished through its spatial properties such as permeability, porosity, hardness and so many other properties, but one of the most recognized characteristics is permeability and porosity [5]. There are many materials in porous media such as man-made materials like cement, natural materials such as rocks, last but not least biological tissues such as bones. Porous media is used in many applications in science and engineering fields. The flow of fluids through the porous medium faces movement's obstruction due to the friction of the fluid with the walls of the porous medium [5]. AL-Khafajy et al. in [3], studied variable viscosity effects of mass transfer on the MHD oscillatory flow of the Carreau fluid through a porous channel. The most important subject in fluid kinematics through a channel is the magnetic field which is generated from an electric current. It has encouraged other researchers to write about its uses in a variety of science, including the natural and health science. AL-Khafajy in [2], analyze the mathematical model of the effect of peristalsis flow from the MHD of a Jeffrey fluid across a cylindrical polar coordinates system for the slanted porous channel at different temperatures and concentrations with variable

∗Corresponding author: Fatima Khalid Moean

Email addresses: fatimakhalid19981116@gmail.com

Communicated by 'sub etitor'

viscosity for the fluid. The peristaltic flow of a fluid through a channel while a magnetic field is present has been the subject of numerous studies, Reddy in [7], found that when permeability parameter increases, the fluid's velocity increases, but when magnetic parameter increases, the fluid's velocity decreases. Hayat et al. in [4], found out that the fluid's velocity has increased near the flow channel wall when the magnetic parameter has been increased, while the fluid's velocity decreased in the center of the channel. Riaz et al. in [8], found out that the velocity of the fluid decreased with the magnetic parameter. Recently, interest has begun to investigate the effect of the temperature on liquid's moveableness proceed along the channel, as most researchers agree that increasing in the temperature leads to increasing in the fluid's velocity. There is a major concept in biological processes and industrial fluid transport is heat transfer as an example, keep up the body's temperature is one of the most required roles of the cardiovascular system and air that goes into the lungs must also be tempered to the temperature of the body. Mohammed and Hummady in [6], studied the effects of the rotation on heat transfer for peristaltic transport of Sutterby fluid in an asymmetric channel. These studies inspire us to present a mathematical model to analyze the temperature and hydrodynamic peristaltic flow of a Sutterby fluid through a porous wave channel under the influence of rotation.

2. Mathematical Formulation

Consider a peristaltic flow of a Sutterby fluid through a porous wavechannel which the equation for the flow channel wall is $\pm\left(d-\overline{\emptyset}\,sin^2\left(\frac{\pi}{\omega}(\bar{X}-s\bar{t})\right)\right)$ in two-dimensional Cartesian coordinates, where the positive sign represents the upper wall while the negative sign represents the lower wall of the channel. Where d is the average radius of the tube, $\overline{\emptyset}$ is the amplitude of a peristaltic wave, ω is a wavelength, s is a wave propagation speed, and $\bar{t}$ is a time. The fluid is electrically conducted by an external magnetic field, $B=(0,B_0,0)$. The fluid rotates with a uniform angular velocity Ω about the z-axis. Due to the wave motion of the flow channel wall (contraction and relaxation), the fluid moves in the form of a peristaltic flow in the middle of the channel. The basic governing equations of the system are (continuity, momentum, and temperature equation), given by:

$$\nabla.\bar{U}=0. \qquad \text{(continuity equation)} \qquad (1)$$

$$\rho(\bar{U}.\nabla)\bar{U}+\rho\left(\Omega(\Omega\times\bar{U})+2\Omega\times\frac{\partial\bar{U}}{\partial\bar{t}}\right)=\nabla\bar{S}-\frac{\mu}{\bar{K}}\bar{U}+\mu_e.\bar{B}\times\bar{J} \qquad \text{(momentum equation)} \qquad (2)$$

$$\rho c_p(\bar{U}.\nabla)T=H.\nabla^2T+\tau.(\nabla\bar{U})-G(T-T_0) \qquad \text{(temperature equation)} \qquad (3)$$

The definition of Sutterby fluid equation [1] is:

$$\bar{S}=-\bar{p}I+\tau$$

$$\tau=\frac{\mu}{2}\left[\frac{sinh^{-1}(b\dot{\gamma})}{b\dot{\gamma}}\right]^n(\nabla\bar{U}+(\nabla\bar{U})^T). \qquad (4)$$

Here $\bar{U}$ is velocity filed, Ω is the rotation parameter, $\bar{S}$ is the Cauchy stress tensor, $\bar{p}$ is the pressure, I is the unit tensor, τ is the extra stress tensor, μ_0 is the zero shear rate viscosity, and $\dot{\gamma}$ is the second invariant strain tensor which is defined as $\dot{\gamma}=\frac{1}{\sqrt{2}}\sqrt{trac(\nabla\bar{U}+(\nabla\bar{U})^T)^2}$, where $(\nabla\bar{U})$ is a gradient of the fluid velocity, and $(\nabla\bar{U})^T$ is the transpose of the gradient velocity in the Cartesian coordinates system (x,y,z). When $|b\dot{\gamma}|\ll1$, we have $\sinh^{-1}(b\dot{\gamma})\approx(b\dot{\gamma})-\frac{(b\dot{\gamma})^3}{6}$, so that equation (4) become:

$$\tau\approx\frac{\mu}{2}\left[1-\frac{nb^2}{6}(\dot{\gamma})^2\right](\nabla\bar{U}+(\nabla\bar{U})^T). \qquad (5)$$

3. Solution of Problem

Let $\bar{U}_1$ and $\bar{U}_2$ be the respective the components of velocity in the radial and axial directions in the fixed frame, respectively. The equations (1), (2), and (3) may be written as follows:

$$\frac{\partial\bar{U}_1}{\partial\bar{X}}+\frac{\partial\bar{U}_2}{\partial\bar{Y}}=0, \qquad (6)$$

$$\rho\left(\frac{\partial\bar{U}_1}{\partial\bar{t}}+\bar{U}_1\frac{\partial\bar{U}_1}{\partial\bar{X}}+\bar{U}_2\frac{\partial\bar{U}_1}{\partial\bar{Y}}\right)-\Omega\rho\left(\Omega\bar{U}_1+2\frac{\partial\bar{U}_2}{\partial\bar{t}}\right)=-\frac{\partial\bar{p}}{\partial\bar{X}}+\frac{\partial\bar{\tau}_{\bar{X}\bar{X}}}{\partial\bar{X}}+\frac{\partial\bar{\tau}_{\bar{X}\bar{Y}}}{\partial\bar{Y}}-\sigma B_0^2\bar{U}_1-\frac{\mu}{\bar{K}}\bar{U}_1, \qquad (7)$$

$$\rho\left(\frac{\partial \bar{U}_2}{\partial \bar{t}}+\bar{U}_1\frac{\partial \bar{U}_2}{\partial \bar{X}}+\bar{U}_2\frac{\partial \bar{U}_2}{\partial \bar{Y}}\right)-\Omega\rho\left(\Omega\bar{U}_2-2\frac{\partial \bar{U}_1}{\partial \bar{t}}\right)=-\frac{\partial \bar{p}}{\partial \bar{Y}}+\frac{\partial \bar{\tau}_{\bar{Y}\bar{X}}}{\partial \bar{X}}+\frac{\partial \bar{\tau}_{\bar{Y}\bar{Y}}}{\partial \bar{Y}}-\frac{\mu}{\hat{K}}\bar{U}_2, \tag{8}$$

$$\rho c_p\left(\frac{\partial T}{\partial \bar{t}}+\bar{U}_1\frac{\partial T}{\partial \bar{X}}+\bar{U}_2\frac{\partial T}{\partial \bar{Y}}\right)=H\left(\frac{\partial^2 T}{\partial \bar{X}^2}+\frac{\partial^2 T}{\partial \bar{Y}^2}\right)+\frac{\partial \bar{U}_1}{\partial \bar{X}}(\bar{\tau}_{\bar{X}\bar{X}})+\frac{\partial \bar{U}_1}{\partial \bar{Y}}(\bar{\tau}_{\bar{X}\bar{Y}})+\frac{\partial \bar{U}_2}{\partial \bar{X}}(\bar{\tau}_{\bar{Y}\bar{X}})+\frac{\partial \bar{U}_2}{\partial \bar{Y}}(\bar{\tau}_{\bar{Y}\bar{Y}})-G(T-T_0), \tag{9}$$

where, Ω, B_0, σ, $\hat{K}$, ρ, C_p, H, and G refer to "rotation parameter, magnetic field, electric conductivity, permeability, fluid density, specific heat, thermal conductivity, and heat source", respectively. The following relations are for converting from the test frame $(\bar{X},\bar{Y})$ to the wave frame$(\bar{x},\bar{y})$:

$$\bar{u}_1(\bar{x},\bar{y})=\bar{U}_1(\bar{X}-s\bar{t},\bar{Y},\bar{t})\text{-}s,\ \bar{u}_2(\bar{x},\bar{y})=\bar{U}_2(\bar{X}-s\bar{t},\bar{Y},\bar{t}),\ \bar{p}(\bar{x},\bar{y})=\bar{P}(\bar{X}-s\bar{t},\bar{Y},\bar{t}) \tag{10}$$

where $(\bar{u}_1, \bar{u}_2)$ and $(\bar{U}_1, \bar{U}_2)$ are velocity components and $\bar{p}$ is the pressure in a frame wave.

4. Method of Solution

In order to simplify the governing equations of the problem, we might introduce the following dimensionless transformations as follow:

$$\left.\begin{aligned} x=\frac{\bar{x}}{\omega},\ y=\frac{\bar{y}}{d},\ u_1=\frac{\bar{u}_1}{s},\ u_2=\frac{\omega\bar{u}_2}{sd},\ p=\frac{d^2\bar{p}}{\mu\omega s},\ R_e=\frac{\rho sd}{\mu},\ w=\frac{\bar{w}}{d},\ \Psi=\frac{\bar{\Psi}}{ds},\ Q_1=\frac{\overline{Q_1}}{ds},\\ q_1=\frac{\overline{q_1}}{ds},\ \epsilon=\frac{nb^2s^2}{2d^2},\ \delta=\frac{d}{\omega},\ \emptyset=\frac{\bar{\emptyset}}{d},\ \tau_{xx}=\frac{\omega\,\bar{\tau}_{\bar{x}\bar{x}}}{\mu s},\ \tau_{xy}=\frac{d\bar{\tau}_{\bar{x}\bar{y}}}{\mu s},\ \tau_{yy}=\frac{\omega\,\bar{\tau}_{\bar{y}\bar{y}}}{\mu s},\\ M_e{}^2=\frac{d^2}{\mu}\sigma B_0{}^2,\ H_c=\frac{Gd^2}{\mu c_p},D_a=\frac{\hat{K}}{d^2},\theta=\frac{T-T_0}{T_1-T_0},P_r=\frac{\mu c_p}{H},E_c=\frac{s^2}{c_p(T_1-T_0)} \end{aligned}\right\} \tag{11}$$

where R_e"Reynolds number", $\emptyset$ "amplitude ratio", δ "dimensionless wave number", Ψ "stream function", q_1 "rate of flow", ϵ "Sutterby fluid parameter", D_a "Darcy number", θ "dimensionless temperature", M_e "Magnetic parameter", H_c "heat source parameter", E_c "Eckert number", and P_r "Prandtl number". Substituting equations (10,11) into equations (6-9), we will obtain:

$$\frac{\partial u_1}{\partial x}+\frac{\partial u_2}{\partial y}=0, \tag{12}$$

$$R_e\delta\left((u_1+1)\frac{\partial u_1}{\partial x}+u_2\frac{\partial u_1}{\partial y}\right)-\frac{\rho d^2}{\mu}\Omega^2(u_1+1)=-\frac{\partial p}{\partial x}+\delta^2\frac{\partial \tau_{xx}}{\partial y}+\frac{\partial \tau_{xy}}{\partial y}-\left(M_e^2+\frac{1}{D_a}\right)(u_1+1), \tag{13}$$

$$R_e\delta^3\left((u_1+1)\frac{\partial u_2}{\partial x}+u_2\frac{\partial u_2}{\partial y}\right)-\delta^2\frac{\rho d^2}{\mu}\Omega^2u_2=-\frac{\partial p}{\partial y}+\delta^2\frac{\partial \tau_{yx}}{\partial y}+\delta^2\frac{\partial \tau_{yy}}{\partial y}-\delta^2\frac{1}{D_a}u_2, \tag{14}$$

$$R_e\delta\left((u_1+1)\frac{\partial \theta}{\partial x}+u_2\frac{\partial \theta}{\partial y}\right)=\frac{1}{P_r}\left(\delta^2\frac{\partial^2\theta}{\partial x^2}+\frac{\partial^2\theta}{\partial y^2}\right)+E_c\left(\delta^2\frac{\partial u_1}{\partial x}(\tau_{xx})+\frac{\partial u_1}{\partial y}(\tau_{xy})+\delta^2\frac{\partial u_2}{\partial x}(\tau_{yx})+\delta^2\frac{\partial u_2}{\partial y}(\tau_{yy})\right)-H_c\theta. \tag{15}$$

The component of extra stress of Sutterby's fluid be as the form:

$$\tau_{xy}=\left[1-\epsilon\left\{2\delta^2\left(\frac{\partial u_1}{\partial x}\right)^2+2\delta^2\left(\frac{\partial u_2}{\partial y}\right)^2+\left(\frac{\partial u_1}{\partial y}+\delta^2\frac{\partial u_2}{\partial x}\right)^2\right\}\right]\left(\frac{\partial u_1}{\partial y}+\delta^2\frac{\partial u_2}{\partial x}\right). \tag{16}$$

The associated dimensionless boundary conditions in the wave frame are:

$u_1=-1$ at $y=\pm w=\pm(1-\emptyset\,sin^2(\pi x))$

$\theta=0$ at y=-w=-1+$\emptyset\sin^2(\pi x)$, and $\theta=1$ at $y=w=1-\emptyset\,sin^2(\pi x)$.

Because of the flow channel's structure, we assume the wavelength δ is too small ($\delta \ll 1$). And simplification the equations (13)-(16) by neglecting those parts where this parameter appears, so that we get:

$$-\frac{\rho d^2}{\mu}\Omega^2(u_1+1)=-\frac{\partial p}{\partial x}+\frac{\partial}{\partial y}\tau_{xy}-\left(M_e^2+\frac{1}{D_a}\right)(u_1+1), \tag{17}$$

$$-\frac{\partial p}{\partial y}=0, \tag{18}$$

$$\frac{1}{P_r}\frac{\partial^2\theta}{\partial y^2}+E_c\,\tau_{xy}\left(\frac{\partial u_1}{\partial y}\right)-H_c\theta=0, \tag{19}$$

$$\tau_{xy}=\left[\frac{\partial u_1}{\partial y}-\epsilon\left(\frac{\partial u_1}{\partial y}\right)^3\right]. \tag{20}$$

By substituting equation (20) into equation (17) and equation (19), we obtain:

$$-\frac{\rho d^2}{\mu}\Omega^2(u_1+1)=-\frac{\partial p}{\partial x}+\frac{\partial^2 u_1}{\partial y^2}-3\epsilon\left(\frac{\partial u_1}{\partial y}\right)^2\frac{\partial^2 u_1}{\partial y^2}-\left(M_e^2+\frac{1}{D_a}\right)(u_1+1) \tag{21}$$

$$\frac{\partial^2\theta}{\partial y^2} - P_r H_c \theta = P_r E_c \epsilon \left(\frac{\partial u_1}{\partial y}\right)^4 - P_r E_c \left(\frac{\partial u_1}{\partial y}\right)^2 \quad (22)$$

4.1 Rate of Volume Flow

The instantaneous volume flow rate in fixed coordinates system given by:

$$\hat{Q} = \int_{-W}^{W} \bar{U}_1(\bar{X}\text{-}s\bar{t}, \bar{Y}, \bar{t})d\bar{Y} \quad (23)$$

Using the transformation $(\bar{u}_1(\bar{x},\bar{y})+s)$ into equation (23) and then integrating it, we get:

$$\hat{Q} = \bar{q} + s(W + W) = \bar{q} + 2sW \quad (24)$$

Where $\bar{q} = \int_{-W}^{W} \bar{u}_1(\bar{x},\bar{y})d\bar{y}$

The time mean flow rate over a period $T = \frac{\omega}{s}$ at a fixed position is defined as:

$$\bar{Q} = \frac{1}{T}\int_0^T \hat{Q}\ d\bar{t}. \quad (25)$$

Substituting equation (24) in equation (25), we will obtain:

$$\bar{Q} = \frac{1}{T}\int_0^T (\bar{q} + 2sW)\ d\bar{t} = \bar{q} + 2s(d - \frac{\bar{\emptyset}}{2}). \quad (26)$$

By using (11) into equation (26), we get:

$$dsQ = dsq + 2s(d - \frac{d\emptyset}{2}). \quad (27)$$

The non-dimensional equation (27) has writing as:

$$Q = q + 2 - \emptyset,$$

then $q = Q + \emptyset - 2$.

Where q is the dimensionless volume flow rate in the wave frame has the form:

$$dsq = \int_{-W}^{W} su_1\, d\, dy \quad \rightarrow \quad q = \int_{-W}^{W} u_1\ dy$$

4.2 Velocity Function

The equation (18) shows that p dependents only on x. Equation (21) becomes as:

$$\frac{\partial^2 u_1}{\partial y^2} - Au_1 = \frac{dp}{dx} + 3\epsilon\left(\frac{\partial u_1}{\partial y}\right)^2 \frac{\partial^2 u_1}{\partial y^2} + A, \quad \text{where } A = M_e^2 + \frac{1}{D_a} - \frac{\rho d^2}{\mu}\Omega^2 \quad (28)$$

Because equation (28) is a non-linear differential equation and it's difficult to find an exact solution, so we use the perturbation technique to find the problem solution, as follows:

$$u_1 = u_{10} + \epsilon\, u_{11} + O(\epsilon^2), \quad (29)$$

$$p = p_0 + \epsilon\, p_1 + O(\epsilon^2), \quad (30)$$

$$\Psi = \Psi_0 + \epsilon\, \Psi_1 + O(\epsilon^2), \quad (31)$$

substituting equations (29) and (30) into equation (28), then by equating the similar powers of ϵ, we get the following results displayed as below:

i – Zero-order system (ϵ^0)

$$\frac{\partial^2 u_{10}}{\partial y^2} - A u_{10} = \frac{dp_0}{dx} + A. \tag{32}$$

The associated boundary conditions $u_{10} = -1$ at $y = \pm h = \pm\left(1 - \emptyset sin^2(\pi x)\right)$

ii – First-order system (ϵ^1)

$$\frac{\partial^2 u_{11}}{\partial y^2} - A u_{11} = \frac{dp_1}{dx} + 3\left(\frac{\partial u_{10}}{\partial y}\right)^2 \frac{\partial^2 u_{10}}{\partial y^2}. \tag{33}$$

The associated boundary conditions $u_{11} = 0$ at $y = \pm h = \pm\left(1 - \emptyset sin^2(\pi x)\right)$.

By substituting the solution of equations (32) and (33) in to equation (29), we obtain:

$$u_1 = \frac{e^{\sqrt{A}h}\left(\frac{dp_0}{dx}\right)}{A\left(1+e^{2\sqrt{A}h}\right)}\left(e^{\sqrt{A}y}+e^{-\sqrt{A}y}\right) -$$

$$\frac{A+\left(\frac{dp_0}{dx}\right)}{A}+\epsilon\left(\left(e^{\sqrt{A}y}+e^{-\sqrt{A}y}\right)\left(\frac{1}{8A^2\left(1+e^{2\sqrt{A}h}\right)^4}e^{\sqrt{A}h}\left(\begin{array}{c}-3\left(\frac{dp_0}{dx}\right)^3-6e^{2\sqrt{A}h}\left(\frac{dp_0}{dx}\right)^3-6e^{4\sqrt{A}h}\left(\frac{dp_0}{dx}\right)^3-3e^{6\sqrt{A}h}\left(\frac{dp_0}{dx}\right)^3- \\ 12\sqrt{A}e^{2\sqrt{A}h}h\left(\frac{dp_0}{dx}\right)^3+ \\ 12\sqrt{A}e^{4\sqrt{A}h}h\left(\frac{dp_0}{dx}\right)^3+8A\left(\frac{dp_1}{dx}\right)+24Ae^{2\sqrt{A}h}\left(\frac{dp_1}{dx}\right)+ \\ 24Ae^{4\sqrt{A}h}\left(\frac{dp_1}{dx}\right)+8Ae^{6\sqrt{A}h}\left(\frac{dp_1}{dx}\right)\end{array}\right)\right)-$$

$$\frac{1}{8A^2\left(1+e^{2\sqrt{A}h}\right)^3}e^{-3\sqrt{A}y}\left(\begin{array}{c}3e^{3\sqrt{A}h}\left(\frac{dp_0}{dx}\right)^3-6e^{3\sqrt{A}h+2\sqrt{A}y}\left(\frac{dp_0}{dx}\right)^3-6e^{\sqrt{A}(3h-2y)+2\sqrt{A}y}\left(\frac{dp_0}{dx}\right)^3-6e^{3\sqrt{A}h+6\sqrt{A}y}\left(\frac{dp_0}{dx}\right)^3- \\ 6e^{\sqrt{A}(3h-2y)+6\sqrt{A}y}\left(\frac{dp_0}{dx}\right)^3+3e^{\sqrt{A}(3h-2y)+8\sqrt{A}y}\left(\frac{dp_0}{dx}\right)^3+12\sqrt{A}e^{3\sqrt{A}h+4\sqrt{A}y}y\left(\frac{dp_0}{dx}\right)^3- \\ 12\sqrt{A}e^{\sqrt{A}(3h-2y)+4\sqrt{A}y}y\left(\frac{dp_0}{dx}\right)^3+8Ae^{3\sqrt{A}y}\left(\frac{dp_1}{dx}\right)+24Ae^{2\sqrt{A}h+3\sqrt{A}y}\left(\frac{dp_1}{dx}\right)+ \\ 24Ae^{4\sqrt{A}h+3\sqrt{A}y}\left(\frac{dp_1}{dx}\right)+8Ae^{6\sqrt{A}h+3\sqrt{A}y}\left(\frac{dp_1}{dx}\right)\end{array}\right),$$

where

$$\frac{dp}{dx} = \left(\frac{A^{3/2}(-2+2h+\phi+Q_0)}{2(\sqrt{A}h-\mathrm{Tanh}[\sqrt{A}h])}\right) - \epsilon\left(\frac{\left(A^{3/2}e^{-4\sqrt{A}h}\left(1+e^{2\sqrt{A}h}\right)^4\mathrm{Sech}[\sqrt{A}h]^3\left(\frac{e^{4\sqrt{A}h}\left(12\sqrt{A}h-8\mathrm{Sinh}[2\sqrt{A}h]+\mathrm{Sinh}[4\sqrt{A}h]\right)\left(-\frac{A^{3/2}(-2+2h+\phi+Q_0)}{2(\sqrt{A}h-\mathrm{Tanh}[\sqrt{A}h])}\right)^3}{A^{5/2}\left(1+e^{2\sqrt{A}h}\right)^4}+Q_1\right)\right)}{\left(32(-\sqrt{A}h\mathrm{Cosh}[\sqrt{A}h]+\mathrm{Sinh}[\sqrt{A}h])\right)}\right).$$

4.3 Temperature Function

By substituting the velocity function into the heat equation (22) and then solving the compensation result, we find the temperature function (very long). By drawing the temperature function, we will discuss the effect of the main parameters on the rise or fall of the fluid temperature.

4.4 Pressure Rise, Friction Forces, and Stream Function

Pressure rise Δp_Ω and friction forces F_Ω on the upper and lower walls are defined as follow:

$$\Delta p_\Omega = \int_0^1 \left(\frac{dp}{dx}\right) dx,$$

$$F_\Omega = \int_0^1 h^2 \left(-\frac{dp}{dx}\right) dx.$$

We found the stream function through equation ($\Psi = \Psi_0 + \varepsilon\Psi_1 = \int u_{10}\, dy + \epsilon \int u_{11}\, dy$) and its formula after the solution is:

$$\Psi = -\frac{Ay+\frac{\left(-e^{2\sqrt{A}h-\sqrt{A}(h-y)}+e^{\sqrt{A}(h-y)}\right)\left(\frac{dp_0}{dx}\right)}{\sqrt{A}\left(1+e^{2\sqrt{A}h}\right)}+y\left(\frac{dp_0}{dx}\right)}{A}+\epsilon\left(\frac{1}{8A^{5/2}\left(1+e^{2\sqrt{A}h}\right)^4}e^{-3\sqrt{A}y}\left(-\left(\left(e^{3\sqrt{A}h}+e^{5\sqrt{A}h}-3e^{\sqrt{A}(h+2y)}-\right.\right.\right.\right.$$
$$e^{3\sqrt{A}(h+2y)}-3e^{\sqrt{A}(7h+2y)}+3e^{\sqrt{A}(h+4y)}+3e^{\sqrt{A}(7h+4y)}-e^{\sqrt{A}(5h+6y)}+12e^{\sqrt{A}(5h+4y)}\left(-1+\sqrt{A}(-h+y)\right)+$$
$$12e^{\sqrt{A}(3h+2y)}\left(1+\sqrt{A}(-h+y)\right)+12e^{\sqrt{A}(3h+4y)}\left(-1+\sqrt{A}(h+y)\right)+12e^{\sqrt{A}(5h+2y)}\left(1+\sqrt{A}(h+y)\right)\left(\frac{dp_0}{dx}\right)^3\Big)-$$
$$\left.\left.8Ae^{2\sqrt{A}y}\left(1+e^{2\sqrt{A}h}\right)^3\left(e^{\sqrt{A}h}-e^{\sqrt{A}(h+2y)}+\sqrt{A}e^{\sqrt{A}y}y+\sqrt{A}e^{\sqrt{A}(2h+y)}y\right)\left(\frac{dp_1}{dx}\right)\right)\right).$$

5. Numerical Results and Discussion

In this section, we discuss and graphically analyze the temperature and MHD peristaltic flow of a Sutterby fluid through a porous wavechannel under the influence of rotation, by using the "Mathematica 13" program. This section divided to five subsections: the first one discusses the effect of the parameters on fluid velocity, the second one studies the effect of the parameters on pressure gradient and pressure rise, the third one analyzes the effect of the parameters on Friction Forces, the fourth one analyze the effect of the parameters on temperature, and the final subsection analyzes the effect of the parameters on stream function.

5.1 Velocity Distribution

The Figs. (1a)-(1d) show the effect of parameters $\emptyset$,Ω,Q_0=Q_1,d,M_e,μ,ϵ and D_a respectively, on the distribution of velocity. Fig. (1a), shows that u_1 increases in the middle of the channel, but it decreases near the channel's walls when increases the parameters $\emptyset$ and Ω, respectively. In Fig. (1b), we can see the velocity increases when the flow rate $Q_0 = Q_1$ increases, while the velocity increases in the middle of the channel but decreases near the channel's walls when the average radius d increases. We notice in Fig. (1c), u_1 decreases in the middle of the channel, but increases near the channel's walls when increases the parameters M_e and μ, respectively. Fig. (1d), shows the velocity increases when Sutterby fluid parameter ϵ increases, while the velocity increases in the middle of the channel but decreases near the channel's walls when D_a increases.

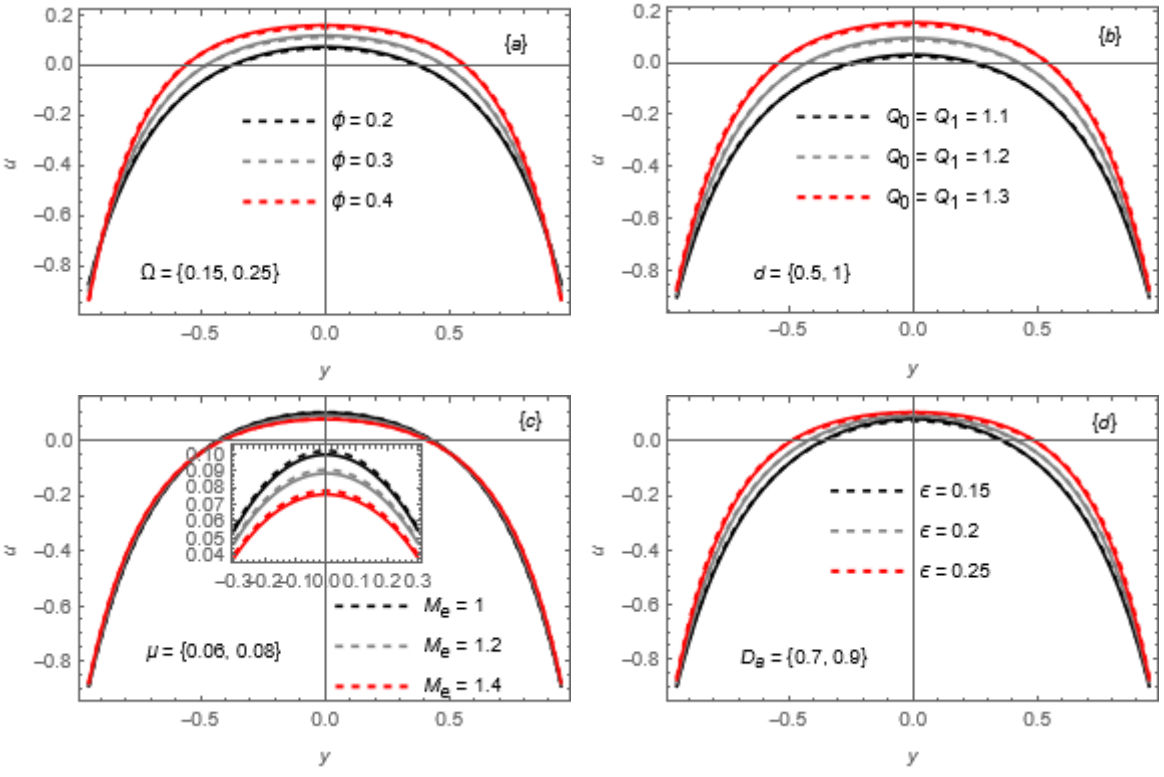

Fig. 1: Variation of the velocity distribution for the following parameters $\{Q_0=Q_1=1.2,\ \emptyset=0.25, \rho=0.8, \mu=0.07, \Omega=0.2, d=0.8, M_e=1.2, D_a=0.8, \epsilon=0.2, x=0.1\}$

5.2 Pressure Distribution

In this subsection, we discussed the influence of parameters $\emptyset,\epsilon,d,\rho,\Omega,\mu,M_e$ and D_a on the pressure gradient dp/dx. In Figs. (2a) and (2b), we can see dp/dx decreases with an increase in the parameters $\emptyset,\epsilon,d$ and ρ, respectively. Fig. (2c), shows the pressure gradient decreases with an increase in the rotation parameter Ω, while dp/dx increases when the fluid's viscosity μ increases. We notice in Fig. (2d), dp/dx increases when the parameter M_e increases, while pressure gradient decreases when D_a increases.

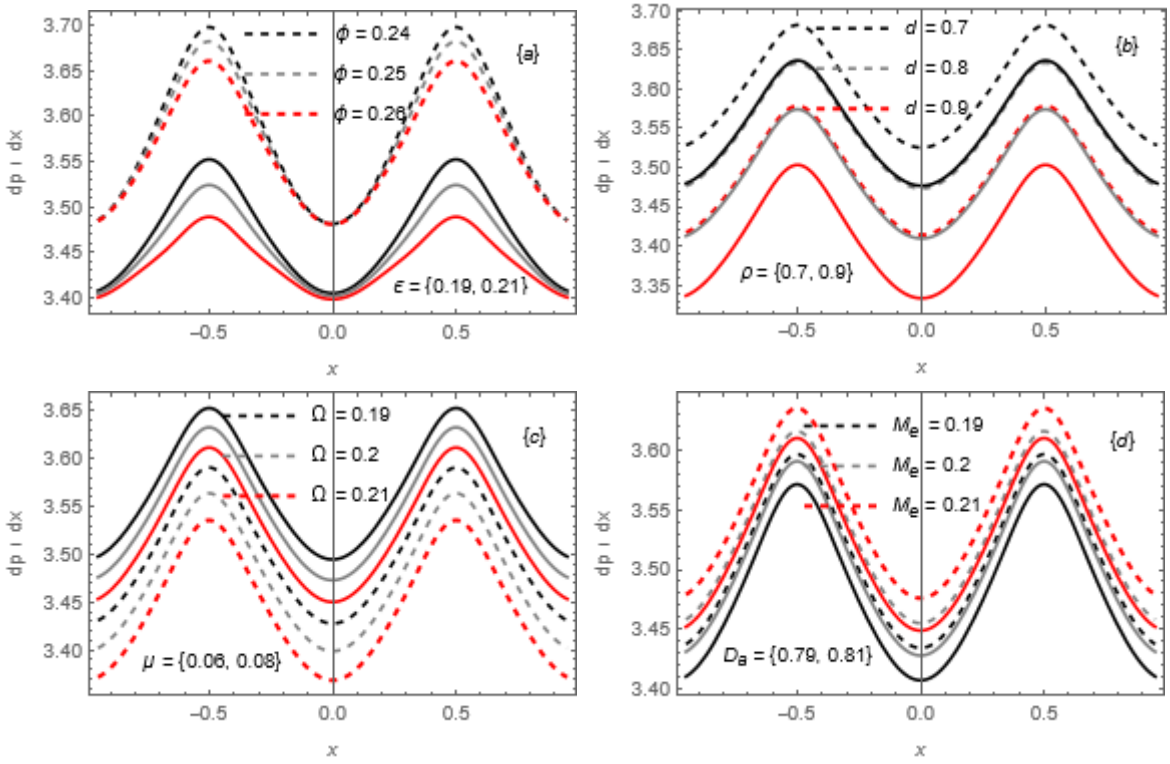

Fig. 2: Variation of the pressure gradient for the following parameters $\{Q_0=Q_1=1.2,\ \emptyset=0.25, \rho=0.8, \mu=0.07, \Omega=0.2, d=0.8, M_e=1.2, D_a=0.8, \epsilon=0.2\}$

Figs. (3a)-(3d) show the effects of the parameters $D_a,\mu,Q_0=Q_1,\rho,\emptyset,\epsilon,M_e$ and d, respectively on the pressure rise Δp_Ω vs. Ω, through the region $1 < \Omega < 1.3$. Fig. (3a), shows that the pressure rise increases when Darcy number increases, while it decreases when μ increases. In Figs. (3b) and (3c), we can see Δp_Ω increases with an increase the parameters $Q_0=Q_1,\rho,\emptyset$ and ϵ. Fig. (3d), shows that Δp_Ω decreases when the magnetic parameter increases, while the pressure rise increases when d increase.

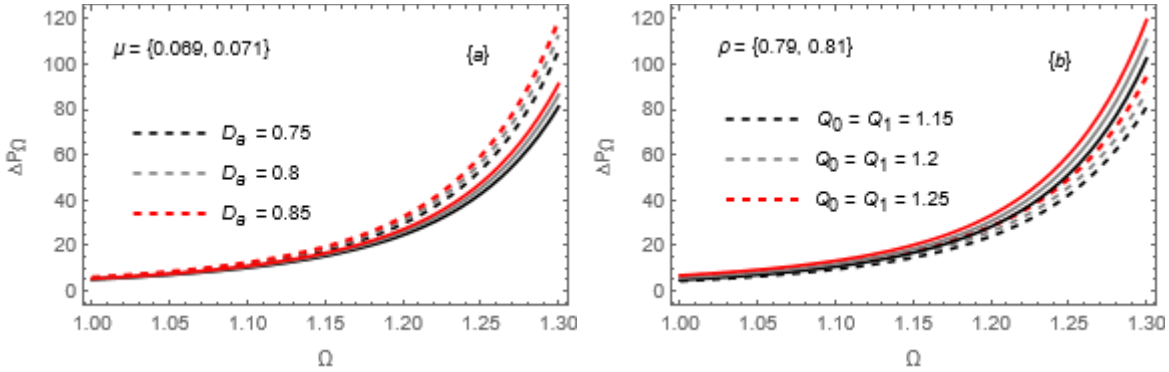

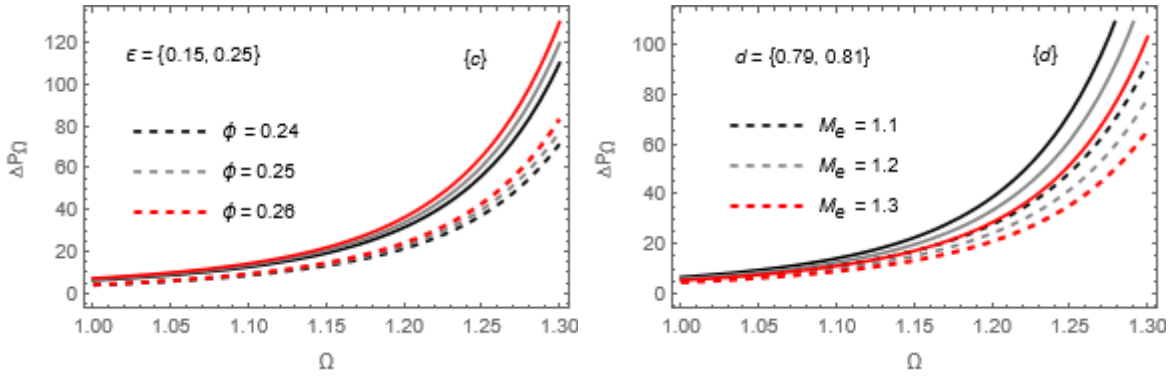

Fig. 3: Variation of the pressure rise for the following parameters $\{Q_0=Q_1=1.2, \emptyset=0.25, \rho=0.8, \mu=0.07, d=0.8, M_e=1.2, D_a=0.8, \epsilon=0.2\}$

5.3 Friction Force Distribution

Figs. (4a)-(4d) shows the effect of parameters D_a,μ,$Q_0=Q_1$,ρ,∅,ϵ,M_e and d on the friction forces F_Ω vs. Ω, through the region $1 < \Omega < 1.3$. Fig. (4a), shows that the friction forces decreases when the parameter D_a increases, while it increases with increasing the fluid's viscosity μ. We can see in Figs. (4b) and (4c), the friction forces decreases when the parameters $Q_0=Q_1$,ρ,∅ and ϵ increases, respectively. In Fig. (4d), the friction forces increases with increasing the parameter M_e, while it decreases when the average radius d increases.

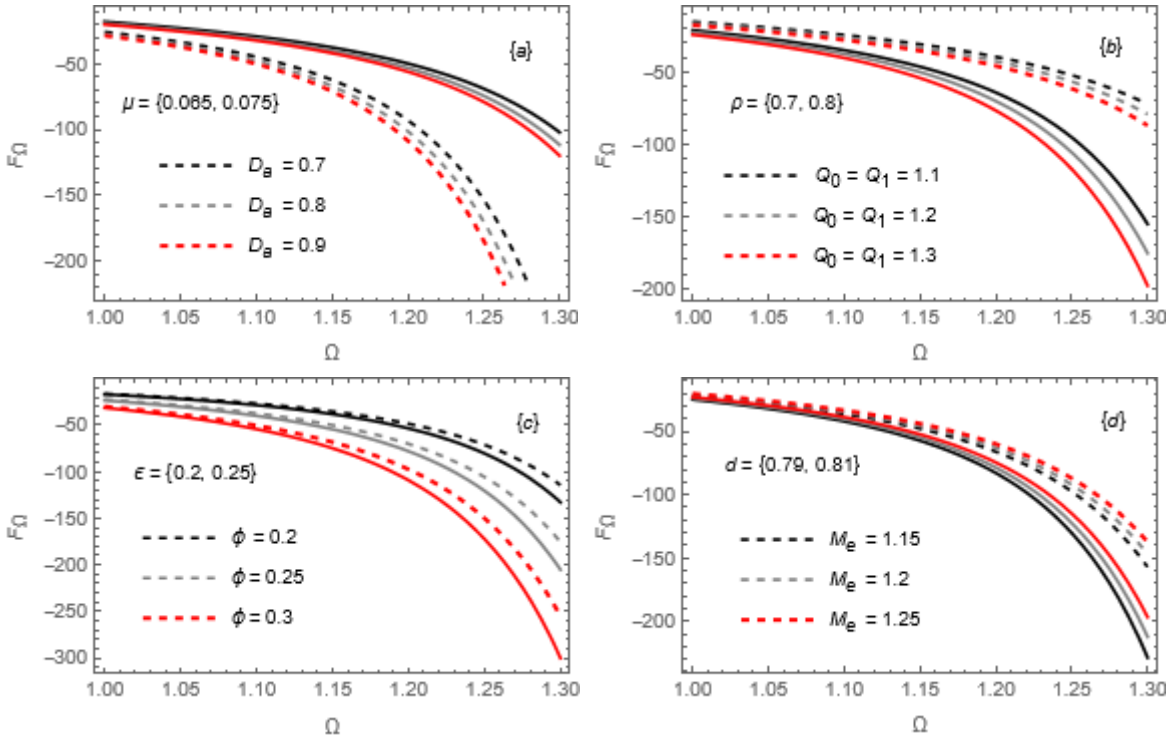

Fig. 4: Variance of the frictional forces for the following parameters $\{Q_0 = Q_1 = 1.2, \emptyset = 0.25, \rho = 0.8, \mu = 0.07, d = 0.8, M_e = 1.2, D_a = 0.8, \epsilon = 0.2\}$

5.4 Temperature profile

Figs. (5a)-(5I) show the effect of parameters $Q_0 = Q_1, \emptyset\ \rho, \mu, \Omega, d, M_e, D_a, \epsilon, E_c, H_c$ and P_r on the temperature vs. y. Fig. (5a), shows that the temperature decreases when parameter $Q_0 = Q_1$ increases. In Fig. (5b), shows the temperature decreases at $y < 0$, while increases at $y > 0$ when ∅ increases. In Figs. (5c) and (5d), we notice that the temperature increases when the fluid's density ρ increases, while the temperature decreases when the fluid's viscosity increases. We can see in Figs. (5e) and (5f), that the temperature increases when the parameters Ω and d

increase, respectively. Figs. (5g) and (5h), show the temperature decreases when the parameters ϵ and M_e increase, respectively. Figs. (5i) and (5j), show that the temperature increases when the parameters D_a and E_c increase, respectively. Fig. (5k), shows that the temperature decreases when parameter H_c increases. In Fig. (5l), we can see that the temperature increases and decreases when the parameter P_a increases.

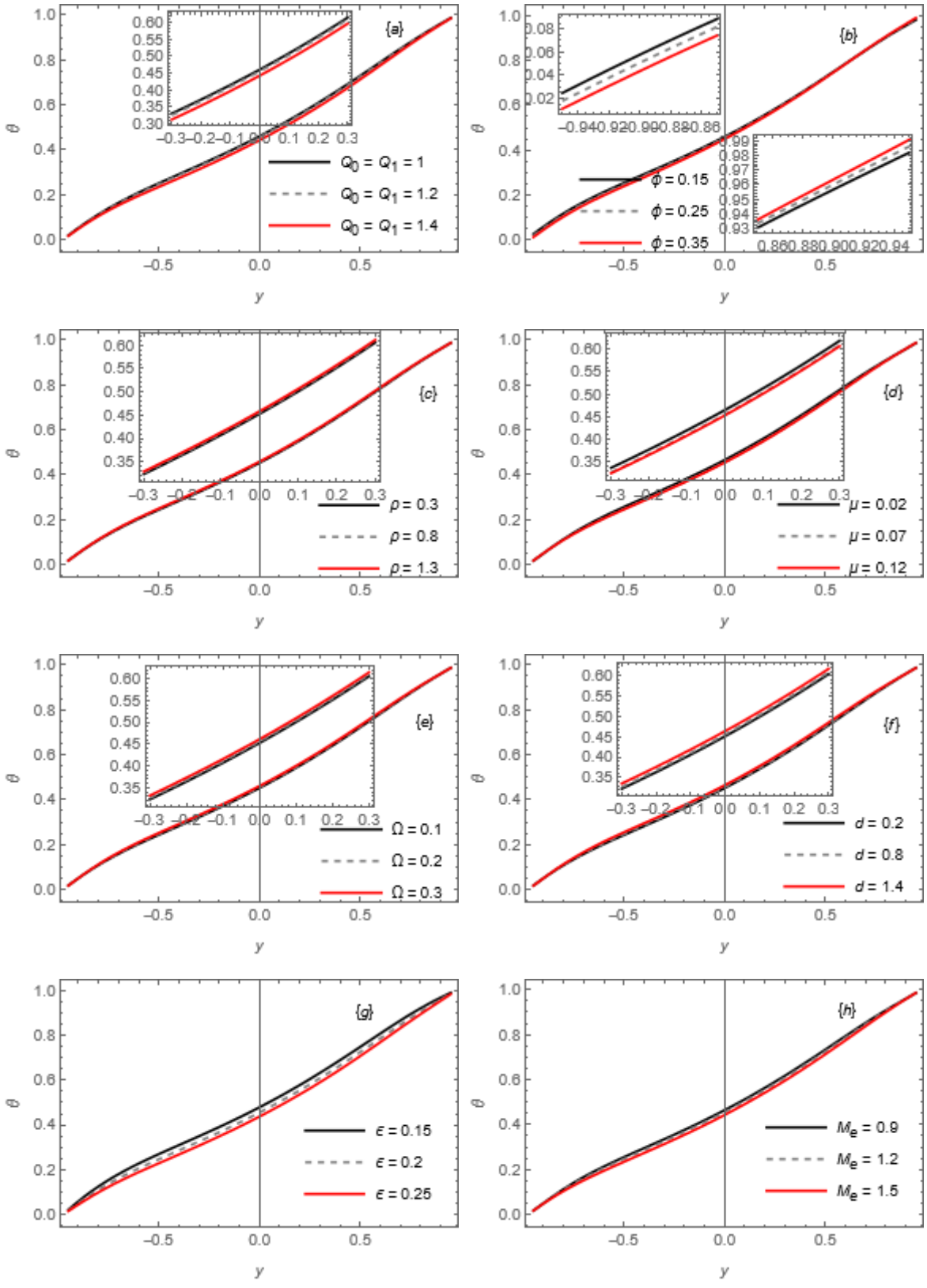

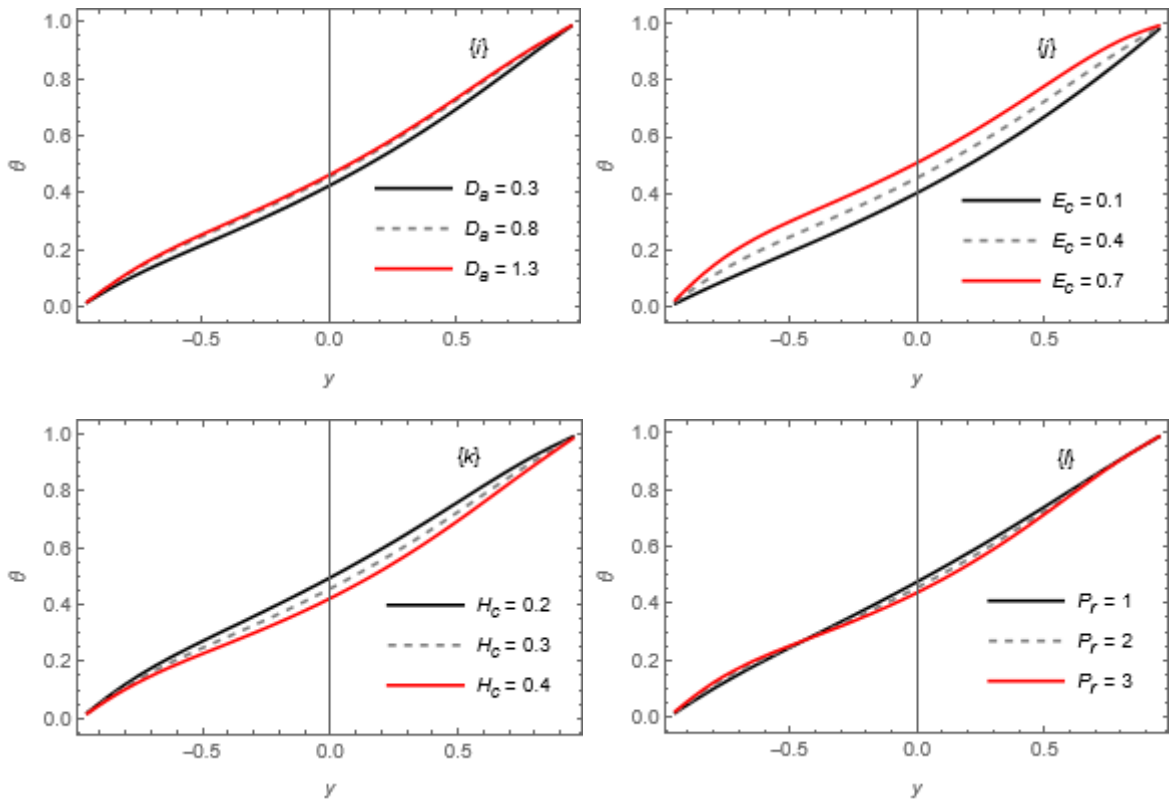

Fig. 5: Variation of the temperature distribution for the following parameters $\{Q_0=Q_1=1.2, \emptyset= 0.25, \rho=0.8, \mu=0.07\ \Omega=0.2, d=0.8, M_e= 1.2, D_a=0.8, \epsilon=0.2, x=0.1, E_c=0.4, H_c=0.3, P_r=2\}$

5.5 Trapping Phenomenon

The creation of in fluid internal bolus by a closed streamline in a fluid flow is known as the trapping phenomenon. In this part we will illustrate the effect of the parameters $Q_0=Q_1, \emptyset, \rho, \mu, \Omega, d, M_e, D_a$ and ϵ on trapped bolus through a porous wavechannel. Figs. (6a)-(6c), show that the trapped bolus has increases at the lower and upper walls of the channel when the parameters $Q_0=Q_1, \emptyset$ and ρ increases. Fig. (6d), shows the trapped bolus decreases when the fluid's viscosity μ increases. In Figs. (6e) and (6f), we can see the trapped bolus increases when the parameters Ω and d increases. Fig. (6g), show that the trapped bolus decreases when the magnetic parameter increases. Figs. (6h) and (6i), show that the trapped bolus increases when the parameters D_a and ϵ increases.

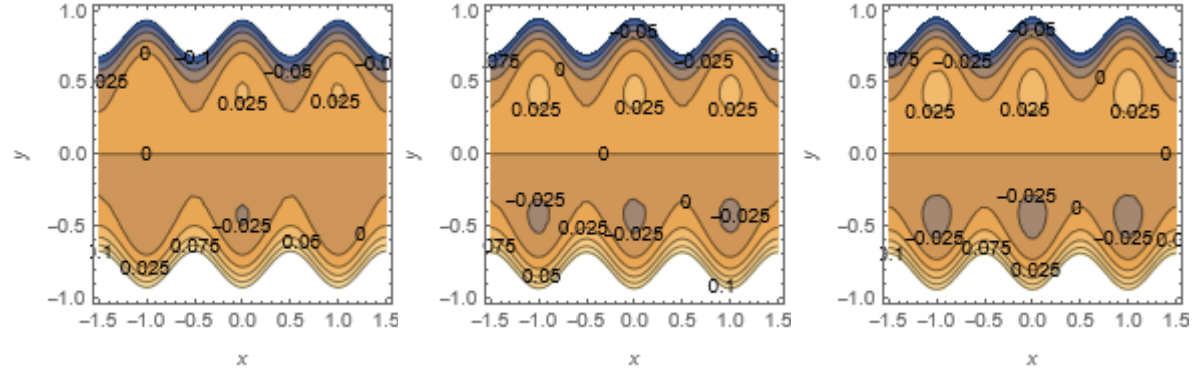

Fig. 6a: Stream function of $Q_0=Q_1=\{1.192, 1.2, 1.208\}$ at $\emptyset=0.25$, $\rho=0.8$, $\mu=0.07$, $\Omega=0.2$, $d=0.8$, $M_e=1.2$, $D_a=0.8$, $\epsilon=0.2$

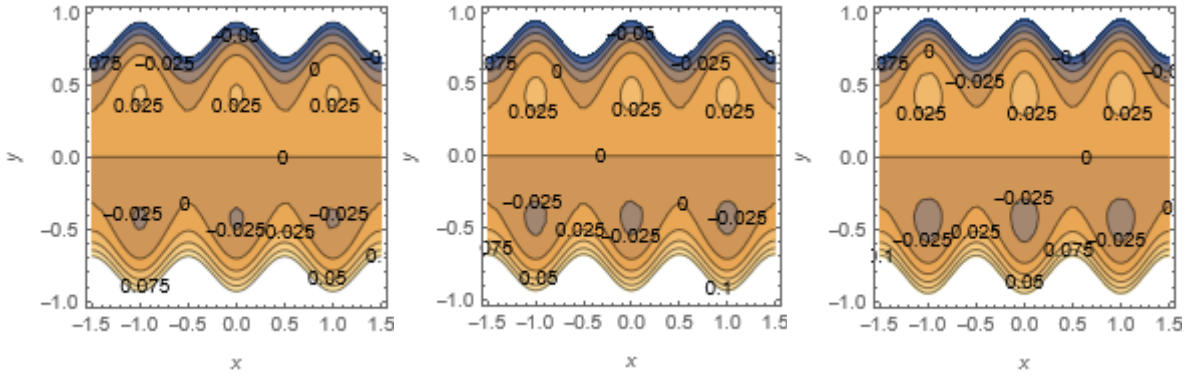

Fig. 6b: Stream function of $\emptyset=\{0.24,0.25,0.26\}$ at $Q_0=Q_1=1.2$, $\rho=0.8$, $\mu=0.07$, $\Omega=0.2$, $d=0.8$, $M_e=1.2$, $D_a=0.8$, $\epsilon=0.2$

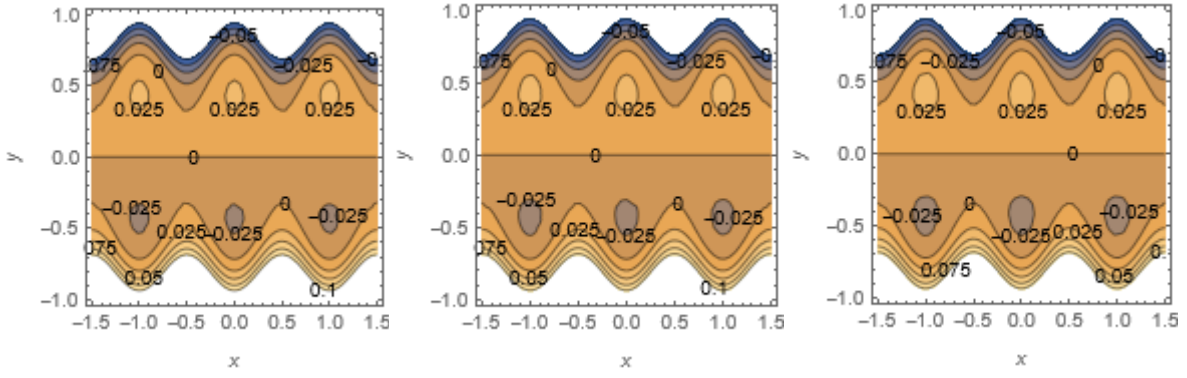

Fig. 6c: Stream function of $\rho=\{0.5,0.9,1.2\}$ at $Q_0=Q_1=1.2$, $\emptyset=0.25$, $\mu=0.07$, $\Omega=0.2$, $d=0.8$, $M_e=1.2$, $D_a=0.8$, $\epsilon=0.2$

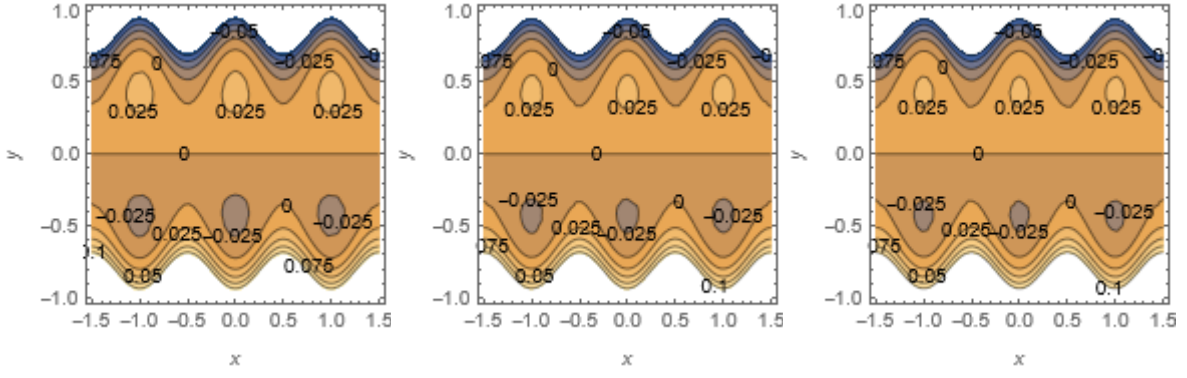

Fig. 6d: Stream function of $\mu=\{0.04,0.07,0.1\}$ at $Q_0=Q_1=1.2$, $\emptyset=0.25$, $\rho=0.8$, $\Omega=0.2$, $d=0.8$, $M_e=1.2$, $D_a=0.8$, $\epsilon=0.2$

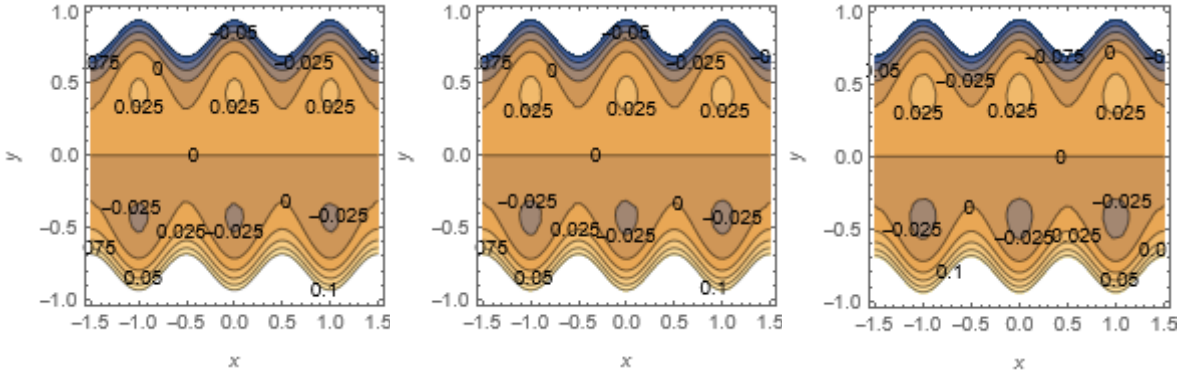

Fig. 6e: Stream function of Ω={0.15,0.2,0.25} at $Q_0=Q_1=1.2$, Ø=0.25, ρ=0.8, μ=0.07, d=0.8,$M_e=1.2$, $D_a=0.8$, ϵ=0.2

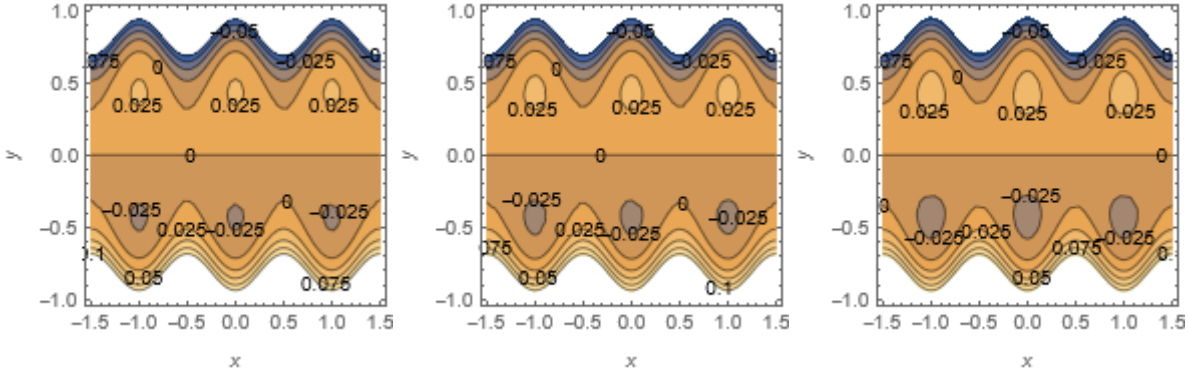

Fig. 6f: Stream function of d={0.5,0.8,1.1} at $Q_0=Q_1=1.2$, Ø=0.25, ρ=0.8, μ=0.07, Ω=0.2,$M_e=1.2$, $D_a=0.8$, ϵ=0.2

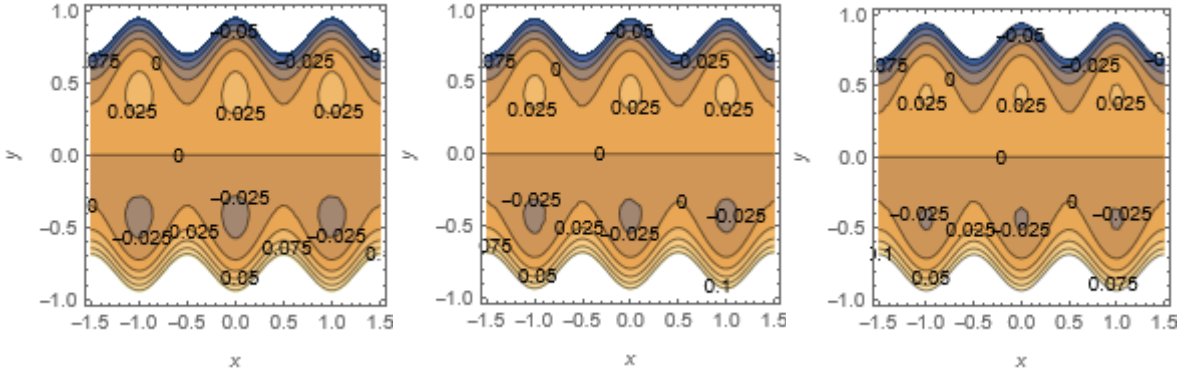

Fig. 6g: Stream function of M_e={1.15,1.2,1.25} at $Q_0=Q_1=1.2$, Ø=0.25, ρ=0.8, μ=0.07, Ω=0.2,d=0.8, $D_a=0.8$, ϵ=0.2

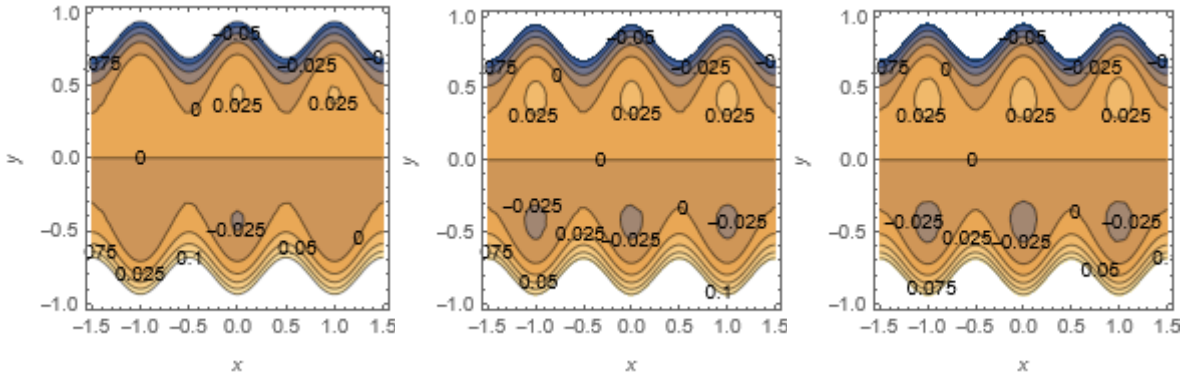

Fig. 6h: Stream function of D_a={0.65,0.8,0.95} at Q_0=Q_1=1.2, ∅=0.25, ρ=0.8, μ=0.07, Ω=0.2,d=0.8, M_e=1.2, ϵ=0.2

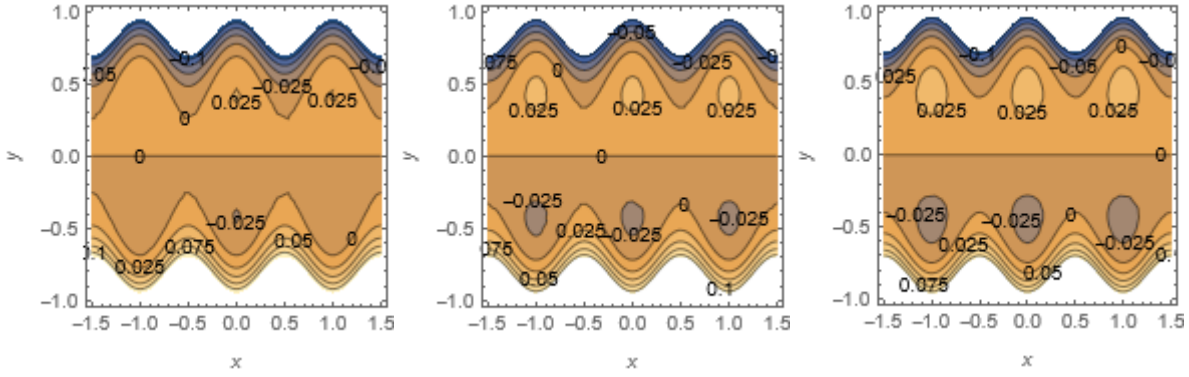

Fig. 6i: Stream function of ϵ={0.18,0.2,0.22} at Q_0=Q_1=1.2, ∅=0.25, ρ=0.8, μ=0.07, Ω=0.2,d=0.8, M_e=1.2,D_a=0.8

6. Conclusion Remarks

In this paper, we analyze the temperature and magnetohydrodynamic (MHD) peristaltic flow of a Sutterby fluid through a porous wavechannel under the effect of rotation. A summary of the above discussed results is as follows:

1. Increasing in the parameters $Q_0 = Q_1$ and ϵ leads to fluid's velocity increases. The velocity of fluid increases in the middle of the channel, but it decreases near the channel's walls when increases the parameters $\emptyset, \Omega, d$ and D_a, while the fluid's velocity decreases in the middle of the channel, but it increases near the channel's walls when the parameters μ and M_e increases.
2. Increasing in the parameters M_e and μ leads to the pressure gradient rise, while by increasing the parameters ∅,ϵ,d,ρ,Ω and D_a leads to the pressure gradient dp/dx decreases.
3. Increasing in the parameters Q_0=Q_1,D_a,ρ,∅,ϵ and d leads to increase in the pressure rise, while by increasing the parameters μ and M_e leads to decrease in the pressure rise.
4. Increasing in the parameters μ and M_e leads to increase in the friction forces, while by increasing the parameters Q_0=Q_1,D_a,ρ,∅,ϵ and d leads to decrease in the friction forces.
5. Increasing in the parameters p,Ω,d,D_a and E_c leads to increase in the temperature, while by increasing the parameters Q_0=Q_1,μ,ϵ,M_e and H_c leads to decrease in the temperature. By increasing the parameters ∅ the temperature decreases at $y < 0$, while increases at $y > 0$. The temperature increases and decreases when the parameter P_a increases.

6. Increasing in the parameters Q_0=Q_1,∅,ρ,Ω,d,D_a and ϵ leads to trapped bolus expanding, while an increase in the parameter μ and the parameter M_e leads to trapped bolus shrinkage.

References

[1] Z. Abbas, M.S. Shabbir, N. Ali, ''Numerical study of magnetohydrodynamic pulsatile flow of Sutterby fluid through an inclined overlapping arterial stenosis in the presence of periodic body acceleration, '' Results in Physics, Vol. 9, pp: 753-762, 2018, doi: https://doi.org/10.1016/j.rinp.2018.03.020

[2] D. G. S. Al –Khafajy, ''Influence of Varying Temperature and Concentration on (MHD) Peristaltic Transport for Jeffrey Fluid through an Inclined Porous Channel,'' Journal of Physics: Conference Series, Vol. 1664, 2020, doi: https://doi.org/10.1088/1742-6596/1664/1/012030

[3] D. G. S. Al-Khafajy ,A. K. Lelo and E. A. Shallal ''Influence of heat carry on magnetohydrodynamics oscillatory flow for variable viscosity Carreau fluid through a porous medium,'' Journal of Interdisciplinary Mathematics, Vol. 24, pp: 519-535, 2021, doi: https://doi.org/10.1080/09720502.2020.1781886

[4] T. Hayat, S. Asghar, A. Tanveer, A. Alsaedi, ''Chemical reaction in peristaltic motion of MHD couple stress fluid in channel with Soret and Dufour effects, '' Results in Physics, Vol. 10,pp: 69-80, 2018, doi: https://doi.org/10.1016/j.rinp.2018.04.040

[5] Q. K. Jawad and A. M. Abdulhadi, ''Influence of MHD and Porous Media on Peristaltic Transport for Nanofluids in An Asymmetric Channel,'' Iraqi Journal of Science, Vol. 64, No. 3, pp: 1344-1360, 2023, doi: https://doi.org/10.24996/ijs.2023.64.3.28

[6] A. A. Mohammed, L. Z. Hummady, ''Influence of Heat Transform and Rotation of Sutterby Fluid in an Asymmetric Channel, '' Iraqi Journal of Science, Vol. 64, No. 11, pp: 5766-5777, 2023, doi: https://doi.org/10.24996/ijs.2023.64.11.24

[7] M.G. Reddy, ''Heat and mass transfer on magnetohydrodynamic peristaltic flow in a porous medium with partial slip, '' Alexandria Engineering Journal, Vol. 55, pp: 1225-1234, 2016, doi: http://dx.doi.org/10.1016/j.aej.2016.04.009

[8] Riaz, A. Zeeshan, S. Ahmad, A. Razaq, M. Zubair, ''Effects of External Magnetic Field on non-Newtonian Two Phase Fluid in an Annulus with Peristaltic Pumping, '' Journal of Magnetics, Vol. 24, pp: 1-8, 2019 .